Molecular Imprinting Technique for Biosensing and Diagnostics

Nenad Gajovic-Eichelmann, Umporn Athikomrattanakul, Decha Dechtrirat, and Frieder W. Scheller

Abstract An introduction into the growing field of molecular imprinting is given, and some principle questions for the design of novel artificial molecular recognition polymers (MIPs) are raised. The limitations of the classical non-covalent imprinting approach are discussed in a brief form. Some novel strategies for the molecular imprinting of macromolecules, especially proteins, are reviewed, as well as new concepts for the integration with transducers and sensors. Two case studies from our own laboratory highlight the question of improving the performance of MIPs by the use of complementary functional monomers and demonstrate a new electrochemical approach to the imprinting of peptides and proteins.

Keywords Electropolymerisation, Functional monomers, Molecular imprinting, Polymers, Protein imprinting

Contents

N. Gajovic-Eichelmann (✉), U. Athikomrattanakul, D. Dechtrirat and F.W. Scheller
Fraunhofer Institute of Biomedical Technology, Am Mühlenberg 13, 14476 Potsdam-Golm, Germany
e-mail: nenad.gajovic@ibmt.fraunhofer.de; nenad.gajovic@ibmt.fhg.de

A. Tuantranont (ed.), *Applications of Nanomaterials in Sensors and Diagnostics*, Springer Series on Chemical Sensors and Biosensors (2013) 14: 143–170
DOI 10.1007/5346_2012_44,
Published online: 8 December 2012

1 General Concept of Molecular Imprinting

Biomimetic, artificial receptor materials with molecular recognition capacity like molecularly imprinted polymers (MIP) have greatly broadened the scope of biosensors and bioanalysis. Novel applications comprise the specific recognition of proteins and peptides [1], nucleotides [2] and catalytically active MIPs [3] besides the well-established imprinting of low-molecular-weight metabolites and drugs [4]. The classical, non-covalent bulk imprinting approach, pioneered by Mosbach [5] as a generalisation of the earlier work by Wulff [6], has turned out the most versatile strategy to the imprinting of small molecules like pesticides, metabolites and drugs [4]. The common basic principle is the mixing of the target molecule (serving as the template) with one or more functional monomers and one or more cross-linking monomers, allowing for the formation of molecular complexes or adducts in solution (pre-arrangement step), prior to the polymerisation step. It is important to realise that the major constituent of nearly all MIPs is the cross-linking monomer, typically making up for 80–90% of the polymer weight. In the resulting porous polymers, being highly cross-linked and rigid, a fraction of the molecular complexes present in the pre-polymerisation mix will be preserved in a quasi-frozen state. In the classical approach, the polymer monoliths are crushed, ground to particles and wet-sieved to achieve a size distribution of typically 25–50 μm. The ground particles may typically have a large surface area of 100–500 $m^2\ g^{-1}$. Upon extraction of the template molecules from the polymer particles, it is believed that specific binding cavities are left behind at the surface, which allow for the selective rebinding of the target [5] (Fig. 1).

1.1 First Considerations When Designing a New MIP

For obvious reasons, the strategy for MIP synthesis will depend on the target to be imprinted.

Is it soluble in common solvents used for MIP preparation? Is it chemically stable? Is it polar or does it bear a charge? Depending on the target, one or few functional monomers will be selected which can form a complex with it. The interactions to be exploited may include ionic interaction, hydrogen bonds, van der Waals forces, hydrophobic interaction, π–π bonds and, as a special case, reversible covalent bonds. The predominant requirement for a proper functional

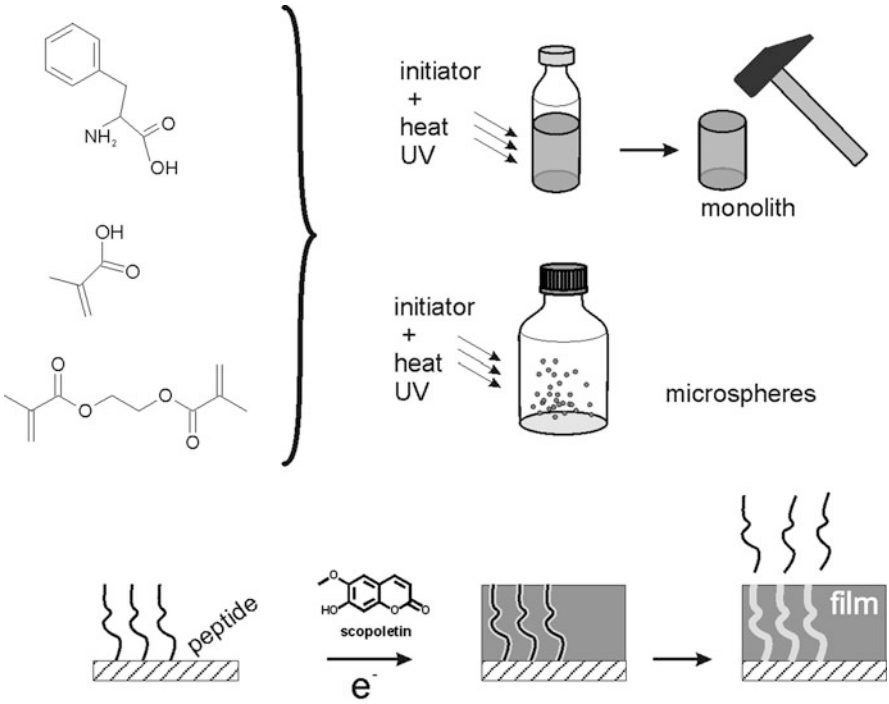

Fig. 1 Schematic of molecular imprinting process, here for the target DL-phenylalanine using methacrylic acid as the functional monomer and EGDMA as cross-linking monomer (*top*: bulk polymer imprinting, intermediate: micro/nanoparticle imprinting). *Lower cartoon* illustrates our novel concept for electrochemical surface imprinting of peptides and proteins

monomer is a high binding constant with the target. It can be determined by methods like NMR titration, isothermal titration calorimetry (ITC) or titration in combination with UV–vis or fluorescence spectroscopy. It is very advisable to determine the binding constant under the same conditions as applied for synthesis, i.e. using the same solvent and the same temperature. The binding constant will provide us with a first hint on the expected performance of the MIP. A few hundreds of monomers are commercially available, with some of them, e.g. methacrylic acid, being used in many applications [4]. If none of these can fulfil the requirements, a synthesis of a custom monomer or a monomer library may be justified. Sellergren's group, amongst others, has recently introduced novel classes of strong binding monomers, which may form stoichiometric complexes even in polar solvents and water [7]. It has become common practice among some MIP researchers to follow a rational design approach [1]. This is often synonymous with selecting the best monomer out of a library of commercial or custom monomers based on molecular modelling results [8]. Several software packages are commercially available for that purpose. Combinatorial libraries of monomers have been developed in analogy to the strategies used in pharma-screening [9].

Once the functional monomer(s) has been found, a cross-linking monomer has to be selected. Although constituting 80–90% of the polymer mass, the cross-linking monomer seems to be less critical for the MIP performance and the vast majority of MIPs use one of these: ethylene glycole dimethacrylate (EGDMA, a polar, divalent cross linker), trimethylolpropane trimethacrylate (TRIM, trivalent cross linker of intermediate polarity), pentaerythritol triacrylate (PETRA, a polar, trivalent cross linker) or divinyl benzene (DVB, an apolar, divalent cross linker). The molar ratios of target:function monomer:cross linker are seldom optimised and most researchers stick to an established recipe (e.g. 1:1:12 or 1:4:20), which seem to give satisfactory results in most cases.

The solvent (porogen) used for polymerisation is critical to the imprinting process: it should be a good solvent for the monomers as well as the target and it should provide a porous polymer. Toluene, acetonitrile and DMSO have often been used. Some studies have been conducted to show that polar solvents will enhance the water compatibility of the MIP [10]. Finally, the cost of the solvent (and its disposal) may dominate the cost of manufacture of an MIP, especially if microspheres or nanoparticles are prepared.

Besides the classical formulation as a bulk monolith, MIPs can be prepared as microspheres [11], nanoparticles or nanogels [12], nanofibres or -filaments [13], inorganic/organic composites [14, 15], thin films [16] or as imprinted hydrogels [17, 18]. The chosen formulation will depend on the application: while ground bulk MIPs lend themselves particularly for solid phase extraction (SPE), thin films or hydrogels may be more easily integrated with biosensors. Inorganic/organic composites may show improved performance in water and nanoparticles or nanofibres may offer higher binding site homogeneity and an improved mass transport, resulting in faster equilibration times. Furthermore, micro-or nanoparticles may be the only option for many “plastic antibody” assay formats, because they will not sediment [19, 20].

Several thousands of MIP-related papers have been published in the last four decades [4], most of them targeting small molecule drugs and metabolites, e.g. antibiotics, steroid hormones, glucose [21] or pesticides like 2,4-D [22] in an organic solvent. The MIP database, run by MJ Whitcombe, is a valuable source of papers and patents on MIPs and can be screened by the target, author or year of publication (www.mipdatabase.com).

1.2 Performance Assessment and Characterisation of MIPs

MIPs are meant to be highly selective adsorbents, so their adsorption properties have to be investigated. All adsorbents are characterised by their adsorption isotherms (for their target and related compounds), specific surface area, porosity and pore size distribution, their solvent compatibility, swelling behaviour, regeneration ability, etc. Adsorption isotherms are most easily determined in batch binding assays [23]. A limited amount of the MIP is added to a dilute solution of the target at

a known starting concentration, and, after the binding equilibrium has been reached, the equilibrium concentration of the target, i.e. the non-bound fraction, is determined by UV–vis spectroscopy, radiolabelled ligands, ^{1}H-NMR titration, FTIR, fluorimetry, ITC or other suitable methods. The adsorbed amount is calculated, and plotted vs. the equilibrium concentration (not the starting concentration!) giving the adsorption isotherm. Adsorption isotherms of MIPs are typically non-linear and complex and will require the use of a scientific software program for quantitative analysis. By fitting the data to a simple (e.g. Langmuir or Freundlich) or more complex isotherm (Bi-Langmuir, Langmuir-Freundlich, etc.), the binding constant and binding capacity can be determined. Batch binding experiments are time and material consuming, however. Alternative methods for the determination of the adsorption parameters have been derived from chromatography. These include zonal analysis (a small amount of the target is loaded on the column and the eluting peak shape is evaluated) and frontal analysis (the column is slightly overloaded with sample, and the breakthrough curve is detected) [24]. These methods typically last less than an hour for one experiment, but it may be expensive to prepare a sufficient amount of MIP to fill the column, and the homogeneous packing of a chromatography column with an irregularly shaped material like ground MIP is very challenging and tedious.

The dominant binding forces in the prepolymer mix and in the polymer were investigated by O'Mahony et al. using ^{1}H-NMR, FTIR and Raman spectroscopy [25, 26]. By these methods they could discern the influence of monomers and solvents on the ionic and hydrophobic interactions, which may eventually lead to a true rational design of MIPs. With the advent of MIP nanomaterials, analytical techniques like Raman spectroscopy, AFM and SPR are commonly used to investigate the release of templates and the rebinding [27].

1.3 MIP-Based Nanomaterials

A large variety of alternative formulations for MIPs have been published in recent years. Protocols for the synthesis of monodisperse microspheres (ca. 1–100 μm in diameter) have been developed to improve the use of MIPs as chromatography materials or as analogues for immunological binding assays. Haginaka has recently reviewed the topic of monodisperse imprinted microparticles as affinity-based chromatography media [28]. Non-porous microspheres will typically have specific surface areas in the order of 10–100 $m^2\ g^{-1}$, which is less than a porous bulk MIP (100–500 $m^2\ g^{-1}$) and may not be sufficient for an adsorbent. Nanospheres (ca. 1–100 nm) will have a much larger surface area and they may be used in binding assays similar to immunoassays, because they do not sediment. The recent developments in the field of micro- and nanosized MIP materials and 2-3D patterned MIP structures have been covered in the review by Tokonami et al. [29]. The recent developments in nanostructured MIPs and core-shell nanoparticle approaches are covered in the review by Guan et al. [12]. Imprinted core-shell

nanoparticles are composed of two types of materials, often a silica nanoparticle core, coated by a polymer shell, and they can combine material properties that are difficult to achieve with straight polymer nanoparticles. Nanofibres or nanofilaments offer a high surface area, can sometimes be prepared directly at sensor surfaces and may be easier to process and handle than nanoparticles [13].

Novel polymerisation strategies, like living free radical polymerisation, including reversible addition-fragmentation chain transfer (RAFT), metal-catalysed atom transfer radical polymerisation (ATRP), nitroxide-mediated polymerisation (NMP) for the preparation of defined MIP nanomaterials, have been reviewed by Chen et al. [30]. In a recent study, Oxelbark et al. have compared the performance of bupivacaine-imprinted polymers, which were prepared as crushed monoliths, microspheres, silica-based composites and capillary monolith formats, by chromatographic methods [14]. Interestingly, the imprinting factors were the highest and the aqueous compatibility was best with the classical ground monolith particles (i.e. bulk imprinting) approach. From a commercialisation perspective, ground monolith particles may be very interesting, because they can be produced at low cost, with little starting materials and solvents, and inexpensive processing (grinding, wet-sieving, etc.).

1.4 Classical and Novel Applications of MIPs

Molecularly imprinted solid phase extraction materials (MISPE) have been in the focus of MIP technology from the beginning and are still the dominating application area in the literature. Extraction of drugs from complex mixtures, metal ions from wastewater, toxins from raw materials, pesticides from soil and water are a few examples of useful applications for MIP sorbents. In their recent review, Bui and Haupt offer an introduction into the design of MISPE protocols, discerning the different strategies of selective loading and selective washing, and cover the most recent developments in this field [10].

Modern sensor applications using MIP nanomaterials are reviewed elsewhere [31]. Recently, a number of papers have addressed separation processes with imprinted membranes [32]. Extraction of toxic heavy metal ions like nickel, lead, iron or copper has been demonstrated.

Medical applications of MIPs have been the exception, but a recent paper by Hoshino et al. raised much interest [33]. Melittin, the toxic peptide in bee venom, was imprinted in hydrogel nanoparticles. These MIP particles, when administered to living mice, cleared previously injected melittin and scavenged the immunological reaction, like a real antibody. This groundbreaking paper may pave the way for other medical applications of MIPs.

Commercial MIP applications. The first commercial MISPE solutions are offered by Biotage AB, Sweden, who has recently acquired Lund-based MIP Technologies AB. Their MIP library is marketed as a screening platform (ExploraSep™) for the chemical and pharmaceutical industry and for sample

preparation by solid phase extraction. Group-selective MIPs for acidic, neutral and basic compounds, diols and aromats, are offered in a 96-well plate format, as columns or bulk materials for scale-up.

Semorex Inc., a US- and Israel-based start-up company, has announced the launch of a medical MIP product, a phosphate binding MIP for the treatment of patients with end-stage renal disease, based on the company's proprietary technology.

Polyintell is a French start-up company specialising in MIP-based solid-phase extraction products for various applications in food & feed safety (e.g. mycotoxins), environmental analysis, diagnostics and drugs of abuse detection.

1.5 Limitations of the Non-covalent Imprinting Approach

Although being most versatile, the non-covalent imprinting approach has its limitations: typically only a small fraction of the exposed surface will be imprinted, while the bulk material, which is mainly constituted of the cross-linking monomers, will permit the adsorption of various hydrophobic and polar species, leading to a significant unspecific binding. For a proper assessment of the imprinting effect, it is necessary to determine the binding affinities and binding capacities of the specific as well as the unspecific binding sites, e.g. by batch binding experiments and proper evaluation of the resulting binding isotherms.

The second problem is the heterogeneity of specific binding sites, resulting in a wide distribution of adsorption energies and, hence, binding affinities among the population of binding sites. It is a consequence of the template-monomer complexes in the pre-polymerisation mix being more or less ordered, resulting in a variation in the number and orientation of weak interactions between them [34]. This inherent heterogeneity leads to complex binding isotherms, and ultimately to a decreased selectivity in extraction, sensing or chromatography applications. This characteristic can be improved by the covalent imprinting approach, pioneered by Wulff [35], which utilises reversible, covalent bonds between templates and functional monomers. Such adducts are generally more stable than their non-covalent counterparts, with negligible dispersion in bond energies. Utilising this approach and using a boronic acid derivative as the covalent receptor group, our group was able to synthesise an MIP with uniform binding sites for D-fructose, a common monosaccharide [36]. The concept of stoichiometric imprinting tries to combine the advantages of covalent imprinting with non-covalent synthesis protocol [37].

Another problem, especially with crushed monolith preparations of MIPs, is the incomplete extraction of the template after polymerisation. A significant portion of the template molecules (up to 50%) will be deeply entrapped inside the bulk material, and may eventually leach out, compromising the performance in many analytical applications like SPE and chromatography. Ellwanger et al. have explored different extraction methods including Soxhlet and microwave-assisted extraction (MAE) for the complete removal of the template from a clenbuterol-imprinted

polymer and found MAE to be superior to the commonly used Soxhlet extraction for this particular target [38]. In general, templates can be more easily extracted from MIPs prepared in the form of nanoparticles or thin films [10].

The most severe limitation, however, is the often poor (and virtually unpredictable) water compatibility of most MIPs prepared by the conventional non-covalent technique. Many, if not most, MIPs are meant to be used in purely aqueous solutions or mixtures of organic solvents and buffer. But only few conventional MIPs have been shown to actually work in solvent mixtures with a high water content [7, 14, 24] or in purely aqueous solutions [39]. The reasons for this are diverse: although rarely mentioned in the MIP literature, the combined effect of material hydrophobicity and porosity (i.e. roughness) may result in a superhydrophobic, non-wettable surface [40]. Addition of a small fraction (10%) of a polar solvent like methanol reduces the surface energy of water by ca. 30% and may be sufficient to improve the wetting behaviour [3, 36]. Secondly water may compete for hydrogen bonds and van der Waals bonds at the imprinted binding sites, effectively excluding the target molecules from the interaction sites [10].

1.6 Covalent Imprinting Technique for Saccharide Detection

From a historical perspective, covalent molecular imprinting is an even older technique than non-covalent imprinting. The pioneering work of Wulff [37] has paved the way for this technology. Conceptually the only difference is the use of template-functional monomer pairs, which can form one or more reversible covalent bonds. The vast majority of papers have centred around saccharides and other chiral molecules. Boronic acids are well known for their ability to form cyclic diesters with diols and saccharides in highly alkaline solutions. Vinylphenylboronic acid (VBA) and amino-derivatives thereof have been used as functional monomers for the synthesis of MIPs for saccharides such as D-glucose, D-fructose, D-mannose and derivatives thereof [41]. Wulff et al. have improved the binding constants by using a class of amino-derivatives of VBA as functional monomers, because they have proven to offer higher binding constants at a lower pH than pH 11 [42]. Rajkumar et al. have used this functional monomer for the imprinting of fructosylvalin, the characteristically modified amino acid in glycated haemoglobin (HbA1c) [43] and have used this MIP in a thermometric biosensor [44]. HbA1c is an important biomarker for the assessment of diabetic patients. Using an MIP thermistor as a label-free biosensor system, they could detect fructosylvaline in aqueous solutions with 10% MeOH at pH 8. To improve the performance of boronic acid-based MIPs at a neutral pH, Schumacher and Grüneberger have introduced a novel functional monomer, which is based on the benzoboroxole moiety [36]. Benzoboroxole has been shown to offer much higher binding constants neutral pH with saccharides than VBA [45–47]. In their study with a D-fructose-polymer, the authors showed that their new MIP outperforms the formerly used VBA- or amino-VBA-based polymers at a neutral pH both in terms of binding

capacity and binding affinity [36]. Interestingly, the MIP was highly selective: saccharose, a disaccharide composed of D-glucose and D-fructose, was only weakly bound, and the binding capacity for the enantiomer, L-fructose, was reduced by more than 50%.

1.7 Imprinting of Proteins and Peptides

The previously described techniques of bulk molecular imprinting using non-covalent and covalent target/monomer interactions (and the modifications resulting in micro- or nanoparticulate materials) were shown to produce materials able to selectively recognise a vast number of small target molecules in organic solvents. Obviously, proteins, and to a minor extent peptides, are an extremely important target class in life sciences. Synthetic polymer-based molecular receptors for peptides and proteins would open up a wide range of possibilities for new applications in biotechnology, diagnostics and chemistry, complementary to and extending beyond the scope of current antibody technology. Protein purification in one step, diagnostic tests in aggressive sample matrices and novel biosensors are some of the novel possibilities. Therapeutic MIPs in analogy to therapeutic antibodies may eventually have the largest commercial potential of all MIP applications. Compared to small molecule imprinting, where the first commercial products have recently entered the market, we have just taken the first steps along the road towards "plastic antibodies" able to recognise any desired protein. Macromolecular targets like proteins pose additional difficulties, and classical imprinting approaches have mostly failed to deliver satisfactory results. Several reasons for this have been identified: proteins are in general not compatible with organic solvents and will quickly denature in prepolymerisation mixtures based on organic solvents as porogens. Furthermore, mass transport of macromolecules may be prohibitively slow in a highly cross-linked polymer matrix. As a consequence, the protein templates may be difficult to remove from the binding pockets, thus reducing the surface sites available for rebinding [1]. Analogously, rebinding may be too slow for practical applications. Furthermore, the rigid structure of an MIP, lacking the segmental motions of conventional linear polymers, may effectively prevent proteins from entering the specific binding pockets, and unspecific adsorption at the polymer surface may be the predominant binding mode. Finally, the mere availability of sufficient amounts of a highly purified protein target is not granted, and only few proteins are commercially available and low priced.

Several alternative methods have been proposed to address these challenges. An overview of this quickly expanding new field of research can be found in the excellent review by Whitcombe et al. [1]. The technological approaches may be divided into three main strategies: the imprinting of hydrogels as highly flexible, hydrated substitutes for rigid, cross-linked bulk polymers; secondly, the surface imprinting approach, which relies on the imprinting of the polymer surface only, usually applying the polymer as a thin film and the target protein immobilised on a solid surface; and, thirdly, the epitope imprinting approach, which relies on a linear

peptide epitope as the target, mimicking the whole protein to be imprinted. The latter approach does not require the protein as a physical material, but rather the sequence and tertiary structure of the protein have to be known (the absolute minimum requirement would be the N- or C-terminal amino acid sequence). Which of the different strategies works best for a given protein target cannot be predicted a priori.

By applying the bulk imprinting strategy in an aqueous solution comprising dissolved horse myoglobin as the protein template together with the water-soluble neutral functional monomer acrylamide and the cross linker *N*-*N*′-methylene bisacrylamide at a low concentration, Hjerten was able to prepare a protein-imprinted hydrogel [48]. This highly hydrated, sparingly cross-linked and macroporous material proved to be highly selective for horse myoglobin in buffered solutions, as it could discriminate between the target and whale myoglobin, which is a very similar protein. The mechanical stability of the sparingly cross-linker material was insufficient, however. Moreover, being a hydrogel, its swelling properties, and, consequently, its porosity will inevitably depend on the ionic strength and pH of the buffer. Guo et al. improved this system by using macroporous chitosan beads as a semi-rigid matrix, and polymerising haemoglobin-imprinted soft polyacrylamide gel inside the macropores [49]. By combining these two materials they obtained hydrophilic, chemically and mechanically stable protein-imprinted particles in high yield. The hybrid gel beads were shown to selectively adsorb haemoglobin in the presence of BSA, illustrating a low degree of unspecific binding. Because of their hydrogel structure, the equilibrium adsorption lasts more than 10 h, making these materials unfeasible for sensing purposes. Bergmann et al. have recently reviewed the literature on protein imprinting in hydrogels [17].

Surface imprinting using immobilised protein templates proved to be a feasible alternative to bulk imprinting in many cases. Rather than mixing the protein templates and functional monomers in solution, the proteins are immobilised on a solid surface as a monolayer, either by adsorption or by covalent attachment [49]. The pre-polymerisation mix is applied as a thin film to this surface and polymerisation is initiated. The resulting polymer film, after separation of the templated surface, will bear imprinted surface sites. Photopolymerisation or electropolymerisation has been shown to be particularly suited for this method. Lin et al. have successfully imprinted lysozyme, ribonuclease A and myoglobin by μ-contact printing immobilised of the respective proteins at a glass surface, followed by photopolymerisation of a thin polymer film on the solid-state template [50].

Surface imprinting of proteins was also demonstrated using silica nanoparticles as the support for the template, resulting in protein-imprinted nanospheres [51].

In an analogous, electrochemical polymerisation approach, Menaker et al. have electropolymerised poly-3,4-ethylenedioxythiophene (PEDOT) doped with polystyrene sulphonate (PSS) to prepare thin, surface-imprinted polymer microrods (8 μm diameter) directly on the transducer [52]. The microrod morphology was obtained by immobilising the template protein, avidin, inside the pores of a sacrificial track-etched porous polycarbonate membrane. This membrane was pressed onto an

electrode surface and the electropolymerisation (imprinting) step filled up the pores with the PEDOT/PSS polymer. The membrane was dissolved, leaving behind surface-imprinted polypyrrole microrods at the transducer surface. This elegant strategy eliminates the critical step of (mechanically) separating the surface-imprinted film and the templated surface and the need to re-immobilise the surface-imprinted film at the transducer. Rebinding experiments with fluorescence-labelled avidin and BSA as a competitor were conducted in phosphate buffer, and a high selectivity and affinity (ca. 100 nM) of the MIP film was demonstrated.

Whole protein imprinting relies on the availability of a sufficient amount of highly pure protein templates, a precondition that may be difficult to meet. The presence of native proteins during the polymerisation step poses additional constraints: polymerisation can only be achieved in aqueous solution, limiting the choices of functional monomers, cross linkers and initiators to water-soluble species. Thermal initiation is prohibited in most cases and the protein may form covalent bonds with the polymer backbone during the free-radical polymerisation step [1]. Because of these limitations, an alternative imprinting strategy has been proposed that uses a short (4–10 amino acids) peptide epitope, e.g. the C-terminus or N-terminus, as a surrogate for the protein target. This approach, termed epitope imprinting by its inventors, in order to emphasise the similarity to the immunological determinant recognised by an antibody, offers several advantages [53]: the availability of the template protein in a pure form is not necessary, and only the sequence must be known. Peptides are compatible with a number of organic solvents and can be used in conventional MIP pre-polymerisation mixtures. In an evolution of the original concept and combining it with the ideas of surface imprinting, Nishino et al. have applied peptides, immobilised at a glass surface, as a template to achieve an oriented presentation of the epitope [54]. The C-terminal nonapeptide from cytochrome C was imprinted in a 0.5-mm-thick photopolymerised film. After peeling of the film from the surface, the imprinted sites, borne in the surface contacting face of the film, became available for rebinding experiments. The authors demonstrated a stunning selectivity and affinity constant (90 nM) of the binding sites, proving this concept useful for a number of proteins. In a recent paper, the same group has demonstrated an antibody-like in vivo effect of surface-imprinted MIP particles directed against the toxic peptide, melittin [33]. A different approach for the direct imprinting of a peptide or protein in thin, electropolymerised films is developed and described in the following.

2 Non-covalent Imprinting with Two Complementary Functional Monomers: The Case of Nitrofurantoin

2.1 Non-covalent Imprinting of Two Complementary Monomers

The first application of two different functional monomers in the same MIP was reported by Ramström et al. [55]. They revealed that the MIP prepared from a methacrylic acid and 2-vinylpyridine binds the target, an amino acid derivative,

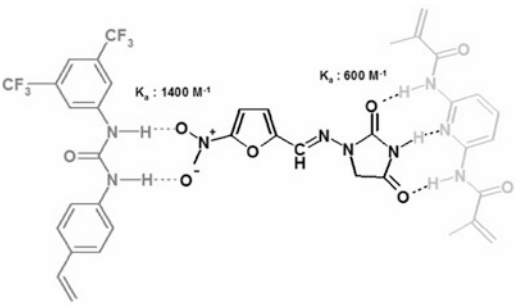

Fig. 2 Ternary complex between nitrofurantoin and two complementary functional monomers (association constants for the binary complexes are indicated)

better than the MIP with only one monomer. In similar works, Takeuchi showed that the selectivity of a triazine-imprinted polymer can be fine-tuned by the relative amounts of MAA and 2-(trifluoromethyl)acrylic acid (TFMAA) [56]. Batch binding experiments showed that a higher proportion of MAA in the polymer favoured the binding of atrazine over ametryn. Several other studies have resorted to commercially available monomers, with the main property being the ionic interaction between the monomer and the target. In a detailed study with nitrofurantoin (NFT), an antibiotic drug, as the model substance, we have explored the potential of combining two complementary, neutral functional monomers in one MIP, starting with custom-synthesised functional monomers [57–59]. NFT belongs to the group of nitrofuran antibiotics and has long been used for the treatment of urinary tract infections in man and husbandry. Because of health risks, it has been banned by the EC for use in husbandry, but it is still commonly used in many food-exporting countries. Because of its quick metabolisation, it was previously not possible to generate antibodies for NFT and to develop sensitive immunoassays. Therefore, an NFT binding MIP is a good option to fill the gap. NFT possesses a neutral nitro-group at the furan ring and a characteristic heteroaromatic hydantoin ring at the opposite site (Fig. 2). Based on a class of monomers originally synthesised for the detection of aromatic carboxy groups [7], a set of three related functional monomers was designed to bind effectively to the aromatic nitro group through two hydrogen bonds, as was demonstrated by ^{1}H-NMR titration of the template-monomer complex [57]. Another monomer was designed to bind the hydantoin moiety of NFT (Fig. 2). Different MIPs were synthesised and characterised using each of the functional monomers alone [58, 59]. The results for an MIP comprising a combination of two complementary functional monomers in one MIP and comparing its performance to the previously reported single functional monomer materials were presented.

2.2 Material and Template Synthesis

2.2.1 Materials

Unless otherwise specified, all chemicals were purchased from Sigma-Aldrich, Germany. 1-Hydroxycyclohexyl phenyl ketone (Irgacure 127) was from Wako,

Japan. Acetonitrile, dimethyl sulphoxide (DMSO) and methanol were obtained from Carl Roth, Germany. All chemicals and solvents were of analytical or HPLC grade. Sep-Pack NH2 cartridges (6 mL, 1 g) were purchased from Waters, UK.

2.2.2 Synthesis of an Analogue Template

The analogue template, carboxyphenyl aminohydantoin (CPAH), was synthesised as follows: 1.091 g (7.6 mmol) of 1-aminohydantoin hydrochloride and 1.185 g (7.9 mmol) of 3-carboxybenzaldehyde were dissolved in 140 mL of absolute dioxane. The dioxane was distilled off by using a vigreux column. The end point was determined by the boiling temperature (88°C azeotrop of dioxane/water; 102°C pure dioxane). After 3 h of refluxing, the yellow precipitate was obtained after cooling down. The solvent was evaporated and a yellow precipitate obtained. Dichloromethane was added for recrystallisation. 1.67 g of the yellow end product was obtained by filtration (94% yield).

2.2.3 Synthesis of the Functional Monomer 2,6-Bis(Methaacrylamido) Pyridine (BMP)

2,6-Diaminopyridine was recrystallised in dichloromethane at 70–80°C under an N2 atmosphere, filtrated and dried before use for synthesis. 5.643 g (50 mmol) of 2,6-diaminopyridine and 10 mL of triethylamine were dissolved in 150 mL tetrahydrofuran. 100 mmol of methacryloyl chloride was added drop wise with vigorous stirring at 0°C over 2 h. The reaction was performed under N2 atmosphere. Then the mixture was heated up to 40°C and refluxed for 1 h. White Et3NHCl precipitate occurred in the solution. The reaction was quenched by adding 100 mL chloroform and 200 mL distilled water into the mixture and the aqueous solution was discarded. The organic layer was washed with sodium hydrogen carbonate (3 × 20 mL), sodium chloride (3 × 20 mL) and dried over sodium sulphate. After filtration, the solvent was evaporated. The concentrated solution was purified by column chromatography (silica gel 60 (particle size), dichloromethane, and chloroform) to give a pale-yellow solid of diaminopyridine derivative (BMP) (2.36 g, 19.3% yield), mp 151–152°C.

2.2.4 Synthesis of the Functional Monomer 1-(4-Vinylphenyl)-3-(3,5-Bis (Trifluoro-Methyl)Phenyl) Urea (VFU)

VFU was synthesised according to the protocol published earlier by Hall et al. [7]. Briefly, to a stirred solution of 4-vinylaniline (20 mmol) in THF (50 mL), 3,5-bis (trifluoromethyl)phenyl isocyanate (20 mmol) in THF (10 mL) was added. The solution was stirred at room temperature overnight. After solvent evaporation the solid residue was recrystallised from ethanol.

2.2.5 Preparation of MIP Based on Two Functional Monomers

The MIP was prepared using the BMP as the first monomer and the urea-based derivative 1-(4-Vinylphenyl)-3-(3,5-bis(trifluoromethyl)phenyl) urea (VFU) as the second monomer. CPAH was used as the template, PETRA as the cross linker, DMSO: acetonitrile (67:33) as the porogen, with a molar ratio of template: monomer1: monomer2: cross linker as 1:1:1:12. According to its composition, the polymer is called MIP-BMP-VFU. Briefly, 0.5 mmol of CPAH, 0.5 mmol of monomer 1 (BMP) and 0.5 mmol of monomer 2 (VFU) were mixed together in 6 mL of DMSO: acetonitrile (67:33) in 10 mL glass vials and incubated for 4 h at 25°C to allow for self-assembly of the host-guest complexes. Then 6 mmol of PETRA and 0.5 wt% of the photoinitiator (Irgacure 127) were added. Each vial was purged with argon for 5 min. After 2 h pre-incubation at 4°C, polymerisation was initiated under ultraviolet light at 366 nm for 6 h. After the polymer monolith was formed, it was broken to coarse pieces with a mortar, and finely ground in a ball mill (Retsch, type S 100). After sieving and washing with hot methanol in a Soxhlet apparatus overnight, most of the template was removed. The course of template removal was monitored with a UV–vis spectrophotometer at 300 nm. The polymer powder was dried for 24 h at 30°C. The non-imprinted control polymer NIP-BMP-VFU was prepared in the same manner as MIP-BMP-VFU but without the template.

The one-functional-monomer MIPs (MIP-BMP, MIP-VFU), meant as reference materials in this study, were prepared according to the same protocol, with the exception that only one functional monomer was used. The overall composition of the polymer changes only little, since the second monomer makes up for only 8% of the polymer dry weight. The idea to increase the cross linker concentration or to add a "neutral" functional monomer was dismissed, because this would also change the polymer composition and cross-linking degree.

2.2.6 Scanning Electron Microscopy and BET Isotherm Porosimetry

Morphologies of the polymers were recorded as scanning electron microscopy (SEM) images with a Gemini Leo 1550 instrument (Carl Zeiss, Oberkochen, Germany) at an operating voltage of 3 keV. The pore parameters and surface areas of the imprinted polymers were measured using a Quantachrome instrument (Automated Surface Area and Pore Size Analyzer, Quadrasorb SI). 30 mg of dry imprinted polymers were degassed at 60°C for 24 h under nitrogen flow to remove adsorbed gases and moisture. The nitrogen adsorption/desorption analysis were performed at 77 K. The surface areas from multi-point N_2 adsorption isotherms were calculated using the Brunauer, Emmett and Teller (BET) equation.

2.2.7 Characterisation of MIP and NIP by Batch Rebinding Studies

The imprinted and non-imprinted polymers were characterised by batch binding experiments to elucidate their equilibrium binding isotherms. Briefly, CPAH or

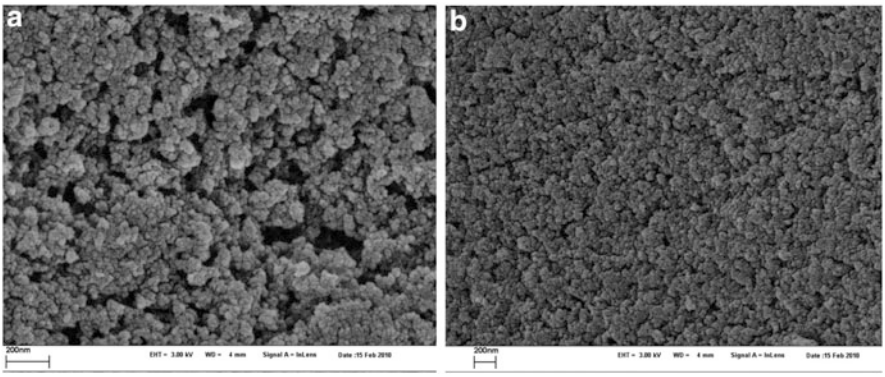

Fig. 3 SEM images of the (**a**) NFT imprinted polymer with two functional monomers (MIP-BMP-VFU) and the (**b**) control polymer NIP-BMP-VFU at 20,000× magnification

NFT solutions (0.001−2.5 mM) were prepared in acetonitrile + 2% DMSO. The DMSO addition was necessary because CPAH and NFT are not soluble in pure acetonitrile. 5 mL of the CPAH or NFT solution was added to 10 mg of polymer in each tube and the mixture was incubated for 24 h at 25°C under stirring. The adsorption isotherms were determined by sedimenting the polymer and measuring the remaining concentration of NFT and CPAH in the supernatant at 300 nm (CPAH) or 370 nm (NFT) using a pre-determined calibration curve for each compound.

2.3 Nitrofurantoin Detection

2.3.1 Morphology and Porosity of MIP and NIP

The surface and porosity of MIP-BMP-VFU and NIP-BMP-VFU were qualitatively compared by electron microscopy. Even at the largest magnification of 20,000× no significant difference could be observed (Fig. 3). From these results, comparable BET surface area data can be expected. Indeed, the surface area for the MIP-BMP-VFU exceeded the respective value for the NIP-BMP-VFU by only 16% (Table 1). Interestingly, the polymers with two functional monomers (both MIP and NIP) had five times increased surface area when compared to the polymers prepared with either one of the functional monomers. Taking into account that the stoichiometric ratio of template to monomer was nearly the same in all pre-polymerisation mixtures, namely 1:1 (with only one functional monomer) and 1:1:1 in the case of two functional monomers, this difference is striking. It is clear evidence for an improved pre-arrangement effect caused by the synergistic action of two

Table 1 BET surface area and porosimetry data for three different MIPS (and control polymer NIPs)

Polymers	Surface area[a] ($m^2\ g^{-1}$)	Total pore volume[b] (mL g^{-1})	Average pore radius[c] (Å)
MIP-BMP	46.46	0.066	29.42
NIP-BMP	34.03	0.061	26.42
MIP-VFU	36.87	0.047	27.30
NIP-VFU	22.92	0.037	24.72
MIP-BMP-VFU	157.4	0.172	35.94
NIP-BMP-VFU	126.9	0.157	32.40

[a]Determined using multi-point BET method
[b]BJH cumulative desorption pore volume of pores with radius less than 19 Å
[c]Average value of pore radius calculated from several models

complementary functional monomers, which may ultimately increase the density of binding sites, i.e. the binding capacity of the new polymer.

2.3.2 Kinetics of NFT Binding

The time dependence of NFT binding to all imprinted and non-imprinted polymers was investigated. Time constants between 0.8 h and 1.2 h were obtained by fitting the adsorption data to a monoexponential growth function in all cases (i.e. the time to reach 67% saturation), with no clear differences between MIPs and NIPs and irrespective of the quite different saturating binding capacities (data not shown). This result indicates that the adsorption proceeds under diffusion limitation and that the pore morphology should be similar for all polymers under study.

2.3.3 Binding Capacity and Affinity of the Imprinted Polymers

In order to determine the imprinting effect and the overall binding capacity for NFT for the two-functional-monomer MIP and the two one-functional-monomer MIPs in this study, the equilibrium binding isotherms were detected and compared (Fig. 4). A qualitative analysis shows an increased binding capacity for the two-functional-monomer MIP (MIP-BMP-VFU) as compared to the other imprinted (MIP-BMP, MIP-VFU) and non-imprinted polymers (NIP-BMP-VFU, NIP-BMP, NIP-VFU). This was consistent with the significantly higher BET surface of this polymer. Table 2 summarises the imprinting factors for all polymer pairs. Obviously the highest imprinting factor of 3.06 (i.e. the ratio of NFT bound by the MIP divided by the amount bound by the respective NIP) was obtained with the two-functional-monomer polymers. The better imprinting effect was also reflected by the highest figure for the binding site occupancy: 8.1% of the theoretically possible binding sites (under the assumption that each template molecule creates one binding site) were actually occupied at a concentration of 1 mM NFT. This is one of the highest

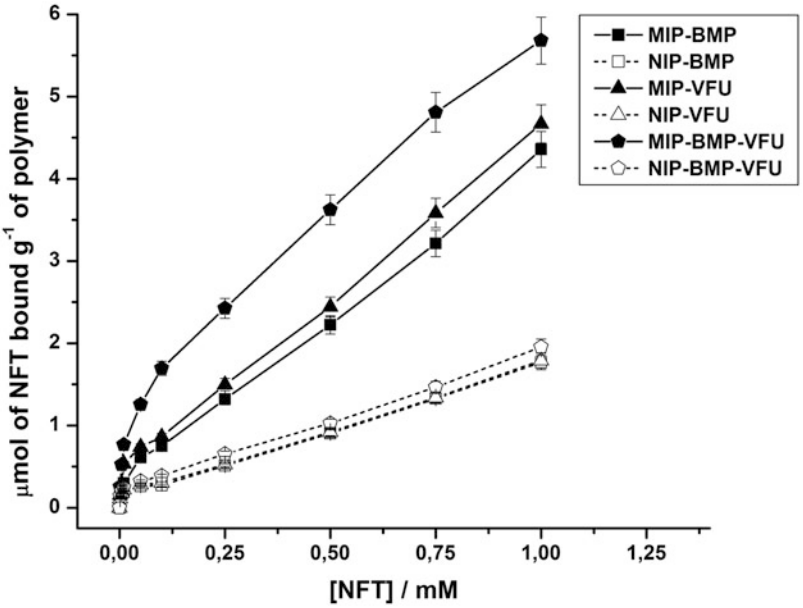

Fig. 4 Binding isotherms for nitrofurantoin at imprinted polymer with two functional monomers (MIP-BMP-VFU) and two MIPs with either one of the two monomers (MIP-BMP, MIP-VFU) and the respective NIP control polymers (condition: 10 mg polymer ad 5 mL solvent (acetonitrile + 2% DMSO))

Table 2 Summary of the imprinting effect for three nitrofurantoin MIPs and control polymers

	Nitrofurantoin		
Polymer	Bound (µmol g^{-1} of polymer)	Imprinting factor	% of binding sites
MIP-BMP	4.380	2.47	5.1
NIP-BMP	1.775		
MIP-VFU	4.670	2.61	5.3
NIP-VFU	1.790		
MIP-2M	5.681	3.06	8.1
NIP-2M	1.854		

$$\text{Imprinting factor} = \frac{\text{Amount of NFT bound by MIP}}{\text{Amount of NFT bound by NIP}}$$

$$\%\ \text{binding sites} = \frac{\text{Amount of NFT bound by MIP}_{\times 100}}{\text{Amount of NFT used for imprinting}}$$

values reported for a bulk imprinted polymer so far, which is even more significant as the actual imprinting has been conducted with the NFT surrogate CPAH, because NFT will deteriorate under the conditions of imprinting.

A Scatchard plot analysis (using a linearised form of the Langmuir isotherm) was performed in order to extract quantitative binding affinity and capacity data,

Table 3 Scatchard analysis of nitrofurantoin binding isotherms at three MIPs

	Nitrofurantoin			
Polymers	K_1 (M^{-1})	B_{max1} (μmol g^{-1})	K_2 (M^{-1})	B_{max2} (μmol g^{-1})
MIP-BMP	79.7	0.82	1.60	5.54
MIP-VFU	121.3	0.92	1.69	5.98
MIP-2M	140.3	1.43	3.16	6.53

under the simplifying assumption of a small population of high-affinity binding sites and a larger population of low-affinity binding sites. The data for both kinds of binding sites are summarised in Table 3, confirming the validity of the hypothesis that the highest-affinity binding sites are present in the two-functional-monomer MIPs. The lower concentration portion of the binding isotherms ($\leq$0.1 mM) was also fitted to a simple Langmuir isotherm using the LMMPro 1.06 software (by C.M. Schulthess) and was in good agreement with the Scatchard analysis (data not shown).

K_1 and B_{max1} are the Langmuir equilibrium constant and the apparent maximum binding capacity for the higher-affinity binding sites (K_2 and B_{max2} are the respective values for the low-affinity binding sites).

In order to improve the affinity of the NFT MIP, a urea-based functional monomer (VFU), capable of donating two hydrogen bonds to the nitro group, and a BMP, capable of donating two and accepting one hydrogen bond from the hydantoin moiety in NFT, was combined in the same polymer. It is thought that the combined actions of the complementary receptor groups are summed up, leading to high-affinity, "multi-point interactions" between the target and the binding pocket inside the MIP. Indeed a synergistic effect was visible as the new polymer outperformed the two reference MIPs in all benchmark tests. Considering the moderate improvement in binding affinity, however, the progress is not satisfactory yet: 15% higher as compared to MIP-VFU, 75% higher as compared to MIP-BMP. We believe that the impact of the porogen (DMSO:acetonitrile in a molar ratio of 67:33) and the cross linker (PETRA) is not yet fully understood with this system and that a rational design approach may help to further improve performance of this polymer. A pronounced group selectivity of the MIPs towards aromatic nitro compounds (VFU) and imido compounds (BMP) has previously been reported by us [59] and a similar selectivity pattern may be expected for the two-functional-monomer MIP.

3 Surface Imprinting of Peptides and Proteins in Ultrathin, Electropolymerised Films

Proteins are among the most interesting targets for MIP sensors: next to the specific extraction of a protein from complex media (e.g. fermentation broth, cell culture supernatant, blood and other biological samples), many immunoassays and other

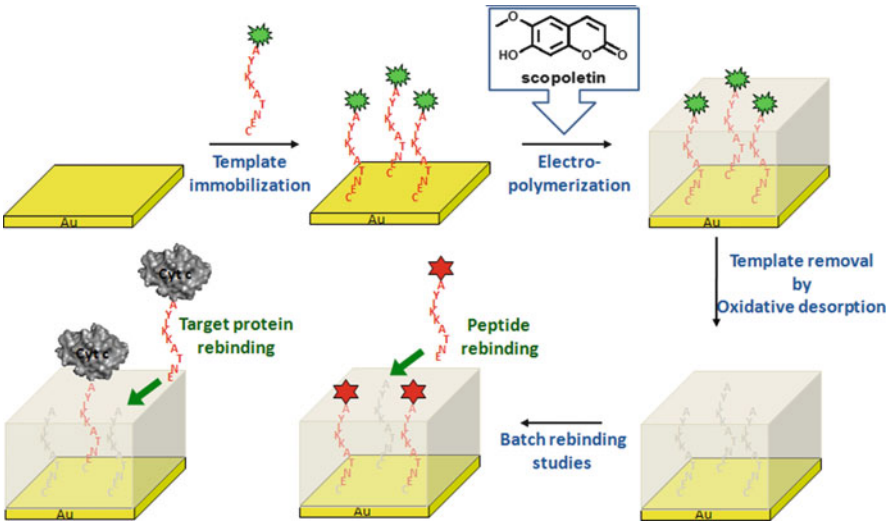

Fig. 5 Electrochemical imprinting of a peptide epitope in an ultrathin electropolymerised polyscopoletin film (complete workflow, schematic)

diagnostic methods rely on the specific detection of a protein. Being relatively unstable macromolecules, conventional MIP protocols cannot be used for the imprinting of a protein. The aim of this chapter is to demonstrate, for the first time, a new molecular imprinting workflow which combines the concepts of epitope imprinting, surface imprinting and electropolymerisation imprinting. The technique is based on electropolymerisation of a non-conductive hydrophilic film [60] in the presence of a chemisorbed peptide template at a gold surface. The template is removed by electrochemical oxidation after the imprinting, leaving behind binding pockets for the peptide. The principle is illustrated in Fig. 5.

3.1 Electrochemical Imprinting

3.1.1 Materials

Scopoletin, cytochrome C (cyt c) from bovine heart, and all other chemicals were purchased from Sigma-Aldrich, Germany, and were of analytical grade or higher. Dy-633-NHS reactive fluorescence dye was from Dyomics GmbH, Germany. TAMRA-labelled peptide template (TAMRA-AYLKKATNEC) and other peptides used were synthesised by Centic Biotec, Germany. Dy-633-labelled peptide (C(Dy-633-M)-AYLKKATNE) was synthesised by Biosyntan (Germany). Ultrapure water from a water purification system (Sartorius, Germany) was used.

Gold-sputtered glass disks (25 mm diameter) with an Au-film thickness of 200 nm were obtained from SSENS, The Netherlands.

3.1.2 Instrumentation

An electrochemical workstation Autolab PGStat30 equipped with GPES software from Eco Chemie, The Netherlands, was used for all electrochemical works. A three-electrode system with a thin-film gold disk, a Pt wire counter electrode, and an Ag/AgCl (1M KCl) reference electrode were used.

Fluorescence imaging was conducted with a Tecan LS Reloaded microarray scanner (Tecan GmbH, Germany) using Array-pro software. Film-thickness determination was conducted with a Nanofilm EP3 imaging ellipsometer (Accurion, Germany) or with a multimode ellipsometer (Multiskop, Optrel GmbH, Germany).

AFM images were taken with a Veeco DI CP II multi-mode AFM instrument in the tapping mode, with standard cantilevers.

3.1.3 Peptide Chemisorption

A peptide, consisting of the C-terminal nonapeptide from bovine heart cytochrome c (residues 97–104 of Cyt c, AYLKKATNE), extended by an extra cysteine at its C-end and labelled with the TAMRA fluorescence dye at its N-terminal end, was synthesised using standard FMOC chemistry and purified by HPLC. The sequence was verified by its mass spectrum.

The adsorption isotherm at the gold surface of the labelled peptide, diluted in 0.1 M phosphate buffer pH 7, was determined in the concentration range from 0.01 mM to 1 mM by fluorescence imaging using a microarray scanner. All scanner settings were kept constant between experiments to maintain reproducibility. The gold surface was purified with a 30-s treatment in hot piranha solution (30% H_2SO_4, 70% H_2O_2. Take care! piranha solution is extremely harmful!) and dried under N_2 before use. Monolayer coverage was achieved at concentrations above 0.1 mM at a fixed incubation time of 3 h at room temperature (data not shown).

To be used as the template, the peptide was chemisorbed to a gold surface from a 0.05 mM solution in 0.1 M phosphate buffer containing 5 mM TCEP, resulting in ca. 60% surface coverage (data not shown). After chemisorption the surface was incubated in phosphate buffered solution pH 7.4 with 0.1% Tween 20 for 20 min, rinsed with water, dried with N_2 and stored in the dark before fluorescence imaging.

3.1.4 Electropolymerisation Imprinting

An aqueous solution of 0.25 mM scopoletin in 0.1 M NaCl solution with 20 mM EDTA was freshly prepared. Electropolymerisation was conducted using a single potential pulse (0.7 V for 5 s, then 0 V for 15 s) without prior deoxygenation of the solution. The gold disk was rinsed with water, dried with N_2 and stored in the dark before fluorescence measurement.

Non-imprinted control films were prepared in the same manner on bare gold surfaces, omitting the template.

3.1.5 Electrochemical Template Stripping

The peptide template was removed by electrochemical oxidation of the thiol (30 s at 1.4 V) in 0.1 M phosphate buffer pH 7. The gold disk with the imprinted film was rinsed with water and incubated in PBS with 0.1% Tween 20 overnight. It was rinsed with water, dried with N_2 and stored dry until used. The percentage of template removal was calculated by comparing the fluorescence intensity of the surface before and after the stripping step.

3.1.6 Batch Rebinding Experiment

The gold disk with the imprinted film was incubated for 18 h in a solution of the Dy633-labelled peptide or in a solution of Dy633-labelled cytochrome c (labelled with the Dy633 according to the standard protocol provided by Dyomics). All solutions were prepared in 0.1 M phosphate buffer, pH 7. A 5-min rinsing step with PBS containing 0.1% Tween-20 was employed to remove nonspecifically bound peptide or protein.

3.2 Surface Imprinting of Peptides and Proteins

3.2.1 Peptide Chemisorption

Monolayer coverage was achieved at concentrations above 0.1 mM at a fixed incubation time of 3 h at room temperature (data not shown). Chemisorption from a 0.05 mM solution in 0.1 M phosphate buffer containing 5 mM TCEP resulted in ca. 60% surface coverage with a high reproducibility (data not shown).

3.2.2 Film Characterisation

The thickness of the electropolymerised poly-scopoletin film as estimated from SPR spectroscopy using the Optrel Multiskope ellipsometer with a 635-nm laser was 4 ± 0.5 nm for the imprinted and 5 ± 0.5 nm for non-imprinted films. The index of refraction was determined as 1.46 and the extinction coefficient as 0.04 (i.e. the film is transparent).

Our attempts to obtain AFM images for the imprinted 4 nm film failed, because of stickiness and AFM artefacts (data not shown). It was, however, possible to image imprinted and non-imprinted poly-scopoletin films of ca. 20 nm thickness

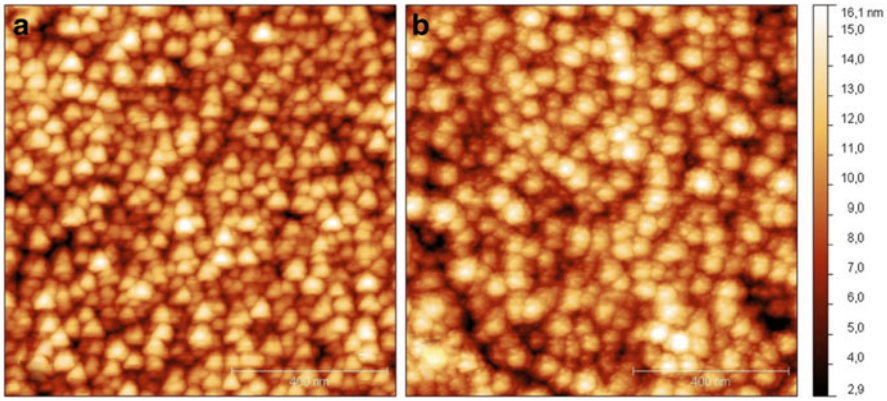

Fig. 6 AFM tapping mode images of a 20-nm-thick (**a**) imprinted and (**b**) non-imprinted poly-scopoletin film

(Fig. 6). Such thick films would not work, because the templates are permanently entrapped in the bulk, and they were prepared merely for the purpose of AFM imaging. These films show a pronounced, grainy structure and a high surface roughness on the same order as the film thickness (ca 16 nm for MIP and NIP). Previous AFM data obtained with 40-nm-thick poly-scopoletin films, prepared by a cyclic voltammetry protocol, consistently showed a continuous, defect-free film with a smooth topography [60]. These preliminary results indicate that the film morphology may be strongly influenced by the deposition protocol favouring a grainy, porous structure with the ultra-thin film obtained by pulse potential deposition.

3.2.3 Template Stripping Efficiency

With the electrochemical oxidation protocol used and based on fluorescence intensity data before and after the template stripping, more than 80% of the chemisorbed template were consistently removed from the 4-nm-thick film (data not shown). This is consistent with the hypothesis that the film thickness is approximately that of the immobilised peptide template.

3.2.4 Peptide Rebinding

The peptide used for the rebinding experiment had the same nonamer sequence as the peptide used as a template, but the C-terminal cystein was omitted in order to avoid chemisorption to the gold, which would confuse the adsorption results. Instead, a cystein was added at the N-terminus. In addition, the peptide was labelled with the deep-red dye Dy633, which could be detected in the red channel of the

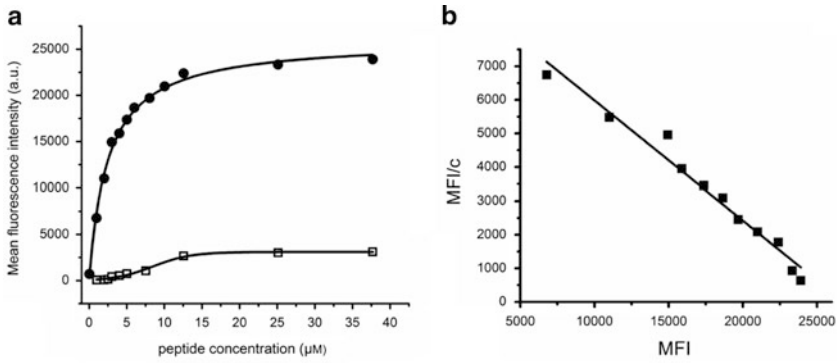

Fig. 7 Peptide rebinding in 0.1 M phosphate buffer at pH 7 to an imprinted poly-scopoletin film (**a**: *filled circles,* **b**: *filled squares*) and a non-imprinted film (**a***: open squares*). (**a**) Binding isotherm extracted from fluorescence images in arbitrary units (*MFI* mean fluorescence intensity). (**b**) Scatchard plot linearisation of binding isotherm (only for the MIP)

microarray reader. In this way, the fluorescence signals were clearly discernible from the signals due to entrapped template peptides (which were labelled with the green fluorescent dye TAMRA). Figure 7a shows the binding isotherm for the peptide (C-(Dy633-M)-AYLKKATNE) rebinding to the imprinted film and the non-imprinted control film. Binding to the imprinted film was characterised by a 10-times higher binding capacity ($\geq$ imprinting factor: 10) as compared to the non-imprinted film and an ideal Langmuir isotherm behaviour. The linear Scatchard plot (Fig. 7b) supports this observation. Most MIPs show a highly non-linear graph in the Scatchard plot, as a result of the heterogeneity in binding sites. As a consequence, we may assume an almost homogeneous population of binding sites, characterised by a single affinity constant (Kd = 2.5 μM). This is an interesting result, as the rather weak interaction between the film and the peptide should be dominated by weak bonds, like hydrogen bonds and van der Waals forces. The apparent homogeneity of binding sites may be a consequence of the site-oriented immobilisation of the template peptide and the homogeneity of the electropolymerised film itself. In contrast to conventional MIPs, electropolymers are prepared from only one monomer, which may explain the apparent homogeneity of binding sites.

3.2.5 Cytochrome C Rebinding

Similar to the rebinding of the AYLKKATNE-peptide, rebinding of fluorescence-labelled cytochrome c holoprotein was conducted in pure phosphate buffer at pH 7. Again the binding capacity of the imprinted film exceeds the value for the non-imprinted one by a factor of 6 ($\geq$ imprinting factor : 6, Fig. 8). These data clearly show that the epitope imprinting of cytochrome c, as demonstrated by Nishino [54], could be reproduced with our electrochemical polymerisation strategy.

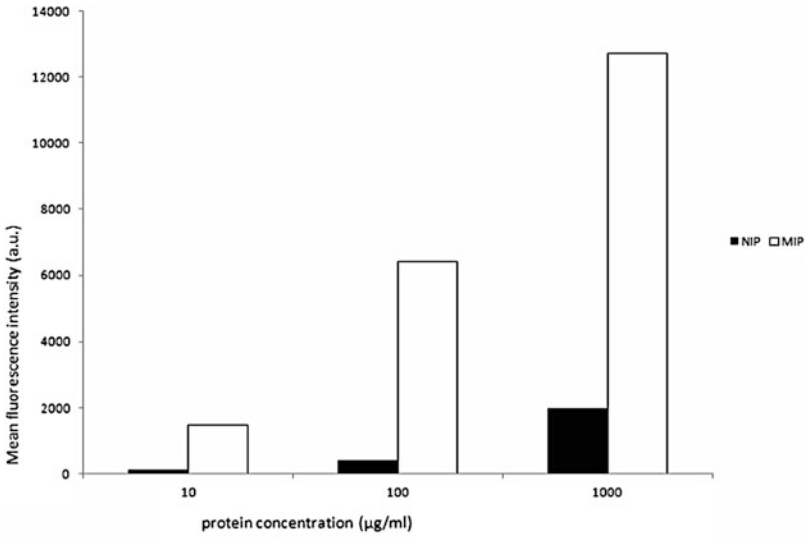

Fig. 8 Cytochrome C rebinding to an imprinted and non-imprinted poly-scopoletin film in 0.1 M phosphate buffer at pH 7, (fluorescence intensity data given in arbitrary units (*MFI* mean fluorescence intensity))

Based on the original Nishino and Menaker approaches, we have developed a workflow for the surface imprinting of thin electropolymerised films with a peptide epitope. Cytochrome c was imprinted by its nonameric C-terminal peptide epitope. The imprinted, hydrophilic poly-scopoletin film possesses a moderately high affinity towards the imprinting peptide (Kd = 2.5 μM), and cytochrome c was detected in buffered solution at the micromolar concentration range in purely aqueous solution. The new technique combines the advantages of the epitope imprinting with the excellent film thickness control that is inherent to electropolymerisation. The imprinted polymer film is grown directly at the electrode surface, including all processing steps. This facilitates the integration with electrochemical, SPR or QCM transducers.

4 Outlook

The field of molecularly imprinted materials is growing at a fast pace, as can be judged from the increasing number of publications and the increasing diversity of methods. This is in contrast to the still quite limited number of commercially available MIPs. Only recently MISPE have become commercially available. Sample preparation by group-selective MISPE for chromatographic analysis seems to be an interesting market niche and may work as an opener for MIP technologies in general. The unique versatility of the molecular imprinting concept and the recent

advances in the rational design of MIP materials, as well as new and unique MIP nanomaterials, will surely promote new applications in biotechnology, analytical chemistry, biosensors and diagnostics. Moreover, the trend towards "green" chemistry and environmentally friendly processes may give an additional momentum for MIP applications in industry. The design of tailor-made MIPs for the detection of proteins in aqueous solutions and complex biological media like blood has become a realistic option in recent years. Significant progress has been achieved by modifications of the classical bulk imprinting approach, resulting in imprinted hydrogel materials with good aqueous compatibility, and by new strategies like surface imprinting and epitope imprinting using immobilised templates. Protein-imprinted electropolymerised thin films can be prepared directly on transducer surfaces with high thickness control using only minute amounts of the protein template. This technique is particularly suited for the functionalisation of SPR, QCM and electrochemical biosensors.

References

1. Whitcombe MJ, Chianella I, Larcombe L, Piletsky SA, Noble J, Porter R, Horgan A (2011) The rational development of molecularly imprinted polymer-based sensors for protein detection. Chem Soc Rev 40:1547–1571
2. Sreenivasan K (2007) Synthesis and evaluation of molecularly imprinted polymers for nucleic acid bases using aniline as a monomer. React Funct Polym 67:859–864
3. Lettau K, Warsinke A, Katterle M, Danielsson B, Scheller FW (2006) A bi-functional molecularly imprinted polymer (MIP): analysis of binding and catalysis by a thermistor. Angew Chem Int Ed 45:6986–6990
4. Alexander C, Andersson HS, Andersson LI, Ansell RJ, Kirsch N, Nicholls IA, O'Mahony J, Whitcombe MJ (2006) Molecular imprinting science and technology: a survey of the literature for the years up to and including 2003. J Mol Recognit 19:106–180
5. Vlatakis G, Andersson LI, Müller R, Mosbach K (1993) Drug assay using antibody mimics made by molecular imprinting. Nature 361:645–647
6. Wulff G (1995) Molecular imprinting in cross-linked materials with the aid of molecular templates. Angew Chem Int Ed 34:1812–1832
7. Hall AJ, Manesiotis P, Emgenbroich M, Quagilia M, de Lorenzi E, Sellergren BJ (2005) Urea host monomers for stoichiometric molecular imprinting of oxyanions. J Org Chem 70:1732–1736
8. Chianella I, Lotierzo M, Piletsky SA, Tothill IE, Chen B, Karim K, Turner APF (2002) Rational design of a polymer specific for microcystin-LR using a computational approach. Anal Chem 74:1288–1293
9. Chen BN, Piletsky S, Turner APF (2002) Design of "keys". Comb Chem High Throughput Screen 5:409–427
10. Bui BTS, Haupt K (2010) Molecularly imprinted polymers: synthetic receptors in bioanalysis. Anal Bioanal Chem 398:2481–2492
11. Mayes AG, Mosbach K (1996) Molecularly imprinted polymer beads: suspension polymerization using a liquid perfluorocarbon as the dispersing phase. Anal Chem 68:3769–3774
12. Guan G, Liu B, Wang Z, Zhang Z (2008) Imprinting of molecular recognition sites on nanostructures and its applications in chemosensors. Sensors 8:8291–8320

13. Linares AV, Vandevelde F, Pantigny J, Falcimaigne-Cordin A, Haupt K (2009) Polymer films composed of surface-bound nanofilaments with a high aspect ratio, molecularly imprinted with small molecules and proteins. Adv Funct Mater 19:1299–1303
14. Oxelbark J, Legido-Quigley C, Aureliano CSA, Titirici MM, Schillinger E, Sellergren B, Courtois J, Irgum K, Dambies L, Cormack PAG, Sherrington DC, De Lorenzi E (2007) Chromatographic comparison of bupivacaine imprinted polymers prepared in crushed monolith, microsphere, silica-based composite and capillary monolith formats. J Chromatogr A 1160:215–226
15. Yilmaz E, Haupt K, Mosbach K (2000) The use of immobilized templates - a new approach in molecular imprinting. Angew Chem Int Ed 39:2115–2118
16. Weetall HH, Rogers KR (2004) Preparation and characterization of mole-cularly imprinted electropolymerized carbon electrodes. Talanta 62:329–335
17. Bergmann NM, Peppas NA (2008) Molecularly imprinted polymers with specific recognition for macromolecules and proteins. Prog Polym Sci 33:271–288
18. Janiak DS, Kofinas P (2007) Molecular imprinting of peptides and proteins in aqueous media. Anal Bioanal Chem 389:399–404
19. Haupt K, Mayes AG, Mosbach K (1998) Herbicide assay using an imprinted polymer-based system analogous to competitive fluoroimmunoassays. Anal Chem 70:3936–3939
20. Vaihinger D, Landfester K, Krauter I, Brunner H, Tovar GEM (2002) Molecularly imprinted polymer nanospheres as synthetic affinity receptors obtained by miniemulsion polymerization. Macromol Chem Phys 203:1965–1973
21. Piletsky SA, Turner NW, Laitenberger P (2006) Molecularly imprinted polymers in clinical diagnostics. Med Eng Phys 28:971–977
22. Baggiani C, Giraudi G, Giovannoli C, Trotta CF, Vanni A (2000) Chromatographic characterization of molecularly imprinted polymers binding the herbicide 2,4,5-trichlorophenoxyacetic acid. J Chromatogr A 883:119–126
23. Haupt K, Dzgoev A, Mosbach K (1998) Assay system for the herbicide 2,4-dichlorophenoxyacetic acid using a molecularly imprinted polymer as an artificial recognition element. Anal Chem 70:628–631
24. Legido-Quigley C, Oxelbark J, De Lorenzi E, Zurutuza-Elorza A, Cormack PAG (2007) Chromatographic characterisation, under highly aqueous conditions, of a molecularly imprinted polymer binding the herbicide 2,4-dichlorophenoxyacetic acid. Anal Chim Acta 591:22–28
25. O'Mahony J, Molinelli A, Nolan K, Smyth MR, Mizaikoff B (2005) Towards the rational development of molecularly imprinted polymers: ^{1}H NMR studies on hydrophobicity and ion-pair interactions as driving forces for selectivity. Biosens Bioelectron 20:1884–1893
26. O'Mahony J, Molinelli A, Nolan K, Smyth MR, Mizaikoff B (2006) Anatomy of a successful imprint: analysing the recognition mechanisms of a molecularly imprinted polymer for quercetin. Biosens Bioelectron 21:1383–1392
27. Kantarovich K, Tsarfati I, Gheber LA, Haupt K, Bar I (2010) Reading microdots of a molecularly imprinted polymer by surface enhanced Raman spectroscopy. Biosens Bioelectron 26:809–814
28. Haginaka J (2008) Monodispersed, molecularly imprinted polymers as affinity-based chromatography media. J Chromatogr B 866:3–13
29. Tokonami S, Shiigi H, Nagaoka T (2009) Review: micro- and nanosized molecularly imprinted polymers for high-throughput analytical applications. Anal Chim Acta 641:7–13
30. Chen L, Xu S, Li J (2011) Recent advances in molecular imprinting technology: current status, challenges and highlighted applications. Chem Soc Rev 40:2922–2942
31. Shimizu KD, Stephenson CJ (2010) Molecularly imprinted polymer sensor arrays. Curr Opin Chem Biol 14:743–750
32. Park JK, Kim SJ (2004) Separation of phenylalanine by ultrafiltration using D-Phe imprinted polyacrylonitrile-poly(acrylic acid)-poly(acryl amide) terpolymer membrane. Kor J Chem Eng 21:994–998

33. Hoshino Y, Koide H, Urakami T, Kanazawa H, Kodama T, Oku N, Shea KJ (2010) Recognition, neutralization, and clearance of target peptides in the bloodstream of living mice by molecularly imprinted polymer nanoparticles: a plastic antibody. J Am Chem Soc 132:6644–6645
34. Umpleby RJ, Baxter SC, Chen YZ, Shah RN, Shimizu KD (2001) Characterization of the heterogeneous binding site affinity distributions in molecularly imprinted polymers. Anal Chem 73:4584–4591
35. Wulff G, Sarhan H (1972) The use of polymers with enzyme-analogous structures for the resolution of racernates. Angew Chem Int Ed 11:341
36. Schumacher S, Grüneberger F, Katterle M, Hettrich C, Hall DG, Scheller FW, Gajovic-Eichelmann N (2011) Molecular imprinting of fructose using a polymerizable benzoboroxole. Polymer 52:2485–2491
37. Wulff G, Knorr K (2002) Stoichiometric noncovalent interaction in molecular imprinting. Bioseparation 10:257–276
38. Ellwanger A, Karlsson L, Owens PK, Berggren C, Crecenzi C, Ensing K, Bayoudh S, Cormack PAG, Sherrington D, Sellergren B (2001) Evaluation of methods aimed at complete removal of template from molecularly imprinted polymers. Analyst 126:784–792
39. Pan G, Ma Y, Zhang Y, Guo X, Li C, Zhang H (2011) Controlled synthesis of water-compatible molecularly imprinted polymer microspheres with ultrathin hydrophilic polymer shells via surface-initiated reversible addition-fragmentation chain transfer polymerization. Soft Matter 7:8428–8439
40. Lee Y, Ju KY, Lee JK (2010) Stable biomimetic superhydrophobic surfaces fabricated by polymer replication method from hierarchically structured surfaces of Al templates. Langmuir 26:14103–14110
41. Mader HS, Wolfbeis OS (2008) Boronic acid based probes for microde-termination of saccharides and glycosylated biomolecules. Microchim Acta 162:1–34
42. Wulff G, Schauhoff S (1991) Enzyme-analog-built polymers. 27. Racemic resolution of free sugars with macroporous polymers. J Org Chem 56:395–400
43. Rajkumar R, Warsinke A, Möhwald H, Scheller FW, Katterle M (2007) Development of fructosyl valine binding polymer by covalent imprinting. Biosens Bioelectron 22:3318–3325
44. Rajkumar R, Katterle M, Warsinke A, Möhwald H, Scheller FW (2008) Thermometric MIP sensor for fructosyl valine. Biosens Bioelectron 23:1195–1199
45. Hall DG (2005) Boronic acids – preparation and applications in organic synthesis and medicine. Wiley-VCH, Weinheim
46. Rajkumar R, Warsinke A, Möhwald H, Scheller FW, Katterle M (2008) Analysis of recognition of fructose by imprinted polymers. Talanta 76:1119–1123
47. Schumacher S, Katterle M, Hettrich C, Paulke BR, Pal A, Hall DG, Scheller FW, Gajovic-Eichelmann N (2011) Benzoboroxole-modified nanoparticles for the recognition of glucose at neutral pH. Chem Sens 1:1–7
48. Hjerten S, Liao JL, Nakazato K, Wang Y et al (1997) Gels mimicking antibodies in their selective recognition of proteins. Chromatographia 44:227–234
49. Guo TY, Xia YQ, Hao GJ, Song MD, Zhang BH (2004) Adsorptive separation of hemoglobin by molecularly imprinted chitosan beads. Biomaterials 25:5905–5912
50. Lin HY, Hsu CY, Thomas JL, Wang SE, Chen HC, Chou TC (2006) The microcontact imprinting of proteins: the effect of cross-linking monomers for lysozyme, ribonuclease A and myoglobin. Biosens Bioelectron 22:534–543
51. Cutivet A, Schembri C, Kovensky J, Haupt K (2009) Molecularly imprinted microgels as enzyme inhibitors. J Am Chem Soc 131:14699–14702
52. Menaker A, Syritski V, Reut J, Öpik A, Horváth V, Gyurcsányi RE (2009) Electrosynthesized surface-imprinted conducting polymer microrods for selective protein recognition. Adv Mater 21:2271–2275
53. Rachkov A, Minoura N (2001) Towards molecularly imprinted polymers selective to peptides and proteins. The epitope approach. Biochim Biophys Acta 1544:255–266

54. Nishino H, Huang CS, Shea KJ (2006) Selective protein capture by epitope imprinting. Angew Chem Int Ed 45:2392–2396
55. Ramström O, Andersson LI, Mosbach K (1993) Recognition sites incorporating both pyridinyl and carboxy functionalities prepared by molecular imprinting. J Org Chem 58:7562–7564
56. Takeuchi T, Fukuma D, Matsui J (1999) Combinatorial molecular imprinting. Anal Chem 71:285–290
57. Athikomrattanakul U, Promptmas C, Katterle M (2009) Synthetic receptors for neutral nitro derivatives. Tetrahedron Lett 50:359–362
58. Athikomrattanakul U, Katterle M, Gajovic-Eichelmann N, Scheller FW (2009) Development of molecularly imprinted polymers for the binding of nitrofurantoin. Biosens Bioelectron 25:82–87
59. Athikomrattanakul U, Katterle M, Gajovic-Eichelmann N, Scheller FW (2011) Preparation and characterization of novel molecularly imprinted polymers based on thiourea receptors for nitrocompounds recognition. Talanta 84:274–279
60. Gajovic-Eichelmann N, Ehrentreich-Förster E, Bier FF (2003) Directed immobilization of nucleic acids at ultramicroelectrodes using a novel electro-deposited polymer. Biosens Bioelectron 19:417–422